Postprint of: Żak A., Krawczuk M., Palacz M., Doliński Ł., Waszkowiak W., High frequency dynamics of an isotropic Timoshenko periodic beam by the use of the Time-domain Spectral Finite Element Method, JOURNAL OF SOUND AND VIBRATION, Vol. 409, (2017), pp. 318-335, DOI: 10.1016/j.jsv.2017.07.055

© 2017. This manuscript version is made available under the CC-BY-NC-ND 4.0 license
http://creativecommons.org/licenses/by-nc-nd/4.0/

High frequency dynamics of an isotropic Timoshenko periodic beam by the use of the Time-domain Spectral Finite Element Method

A. Żak*, M. Krawczuk, M. Palacz, Ł. Doliński, W. Waszkowiak

Gdansk University of Technology, Faculty of Electrical and Control Engineering, ul. Narutowicza 11/12, 80-234 Gdansk, Poland

Abstract

In this work results of numerical simulations and experimental measurements related to the high frequency dynamics of an aluminium Timoshenko periodic beam are presented. It was assumed by the authors that the source of beam structural periodicity comes from periodical alterations to its geometry due to the presence of appropriately arranged drill-holes. As a consequence of these alterations dynamic characteristics of the beam are changed revealing a set of frequency band gaps. The presence of the frequency band gaps can help in the design process of effective sound filters or sound barriers that can selectively attenuate propagating wave signals of certain frequency contents. In order to achieve this a combination of three numerical techniques were employed by the authors. They comprise the application of the Time-domain Spectral Finite Element Method in the case of analysis of finite and semi-infinite computational domains, damage modelling in the case of analysis of drill-hole influence, as well as the Bloch reduction in the case of analysis of periodic computational domains. As an experimental technique the Scanning Laser Doppler Vibrometry was chosen. A combined application of all these numerical and experimental techniques appears as new for this purpose and not reported in the literature available.

Keywords: structural periodicity, Bloch reduction, spectral finite element method, natural frequencies, frequency band gaps, wave propagation

1. Introduction

Despite their finite dimensions structural elements of periodically changing or varying geometry and/or material properties may be considered as being periodic structures. In a similar manner to idealised periodic structures that can be characterised by periodic boundary conditions or infinite dimensions, real periodic structures exhibit the same type of behaviour as predicted theoretically, which manifests itself in the most profound manner in the presence of so-called frequency band gaps in their frequency spectra.

Periodic structures belong to a class of structures the properties of which allow them to be classified as metamaterial structures due to their unusual and engineered properties. Nowadays metamaterials include such materials as: negative refracting index materials, electromagnetic band gap metamaterials, acoustic metamaterials, electrical metamaterials, elastic and structural metamaterials and many more. Thanks to their uncommon physical properties that can be fully controlled during their design and manufacture process, structural elements or whole structures made out of metamaterials may find many interesting potential applications that include cloaking and light filtering in optics [1–3], sound filtering and sound barriers in acoustics [4–7], superconducting in electronics [8–10] or negative Poisson's ratio and Young's modulus in

*Corresponding author
Email addresses: arkadiusz.zak@pg.gda.pl (A. Żak), marek.krawczuk@pg.gda.pl (M. Krawczuk), magdalena.palacz@pg.gda.pl (M. Palacz), lukasz.dolinski@pg.gda.pl (Ł. Doliński), wiktor.waszkowiak@pg.gda.pl (W. Waszkowiak)

mechanics [11–13]. For all these reasons metamaterials, and among them periodic structures, stay nowadays at the very centre of interest of many scientists and researchers around the world [14–21].

As already mentioned a special class of metamaterials are acoustic metamaterials that can be characterised by periodical variations of their acoustic properties or geometry resulting in the presence of frequency band gaps. Their unusual behaviour has its source in a coupled interaction between incident, reflected and transmitted acoustic waves. This phenomenon remains well investigated and a great number of research papers on this subject is available in the literature [22].

These research papers can be divided into three general groups, as summarised in Tab. 1, as papers related to analytical, numerical and experimental investigations of periodic structures. Results of analytical investigations can be found in [23–27]. Beside them, those which are related to the application of the Bloch theorem – also known as the Bloch-Floquet theory – can be placed [28–32], together with the results obtained by the use of the Plane Wave Expansion Method (PWEM) [33–37]. However, a great proportion of research papers on periodic structures present results of numerical investigations. These include the application of the Transfer Matrix Method (TMM) [38–42], the Finite Difference Method (FDM) [43–47], the Finite Element Method (FEM) [48–52] or the Frequency-domain Spectral Finite Element Method (FD-SFEM) [53–57]. On the other side the results of experimental investigations on periodic structures can be located, which are reported in [58–62], but it should be emphasised that only few papers can be found on the application of the Scanning Laser Doppler Vibrometry (SLDV) for that purpose [63–67].

Table 1: Synthetic summary of the research papers cited by the authors and related to the investigation of periodic structures.

Type of research	Main research technique employed	References
analytical	mixed	[23–27]
analytical	Bloch theorem	[28–32]
analytical	Plane Wave Expansion Method (PWEM)	[33–37]
numerical	Transfer Matrix Method (TMM)	[38–42]
numerical	Finite Difference Method (FDM)	[43–47]
numerical	Finite Element Method (FEM)	[48–52]
numerical	Frequency-domain Spectral Finite Element Method (FD-SFEM)	[53–57]
experimental	mixed	[58–62]
experimental	Scanning Laser Doppler Vibrometry (SLDV)	[63–67]

At this point it should be noted that the application of the Time-domain Spectral Finite Element Method (TD-SFEM) to investigate high frequency dynamics or wave propagation phenomena in periodic structures has not been widely reported in the available literature. As a computational technique TD-SFEM is far superior not only to classical FEM, in the regime of high frequency dynamic responses [68], but also to the remaining and above mentioned numerical techniques, i.e. TMM, FDM or FD-SFEM. This makes TD-SFEM especially well suited for the analysis of high frequency dynamics, including wave propagation patterns, of various structural elements [69]. On the other side the application of SLDV serves as a perfect complementary experimental technique, especially well fitted to visualise wave propagation patterns, and as a consequence of that, used to verify results of numerical simulations obtained by the use of TD-SFEM.

The authors of the current work aim to present results of numerical simulations obtained just by the use of TD-SFEM and experimental measurements by SLDV that are related to high frequency dynamics as well as wave propagation in an aluminium Timoshenko periodic beam. The source of the beam periodicity is assumed as coming from repeated alterations to its geometry due to the presence of a number of appropriately arranged drill-holes. The authors also take into account the periodic properties of the numerical model itself. These periodic properties come from stress/strain field discontinuities between spectral finite elements and are the source of additional discrete model periodicity [68]. The repeated alterations to the beam geometry lead to the emergence of a set of frequency band gaps in the natural frequency spectrum of the beam. As already mentioned their presence is helpful in the design process of sound filters or barriers. However, the effectiveness of sound filtering or blocking is strongly dependent not only on the number of the frequency band gaps present, but also on their width and location in the frequency spectrum. The authors want to demonstrate that the number of the frequency band gaps as well as their location and width can be controlled

MOST WIEDZY Downloaded from mostwiedzy.pl

by the number of drill-holes and their diameters, thus influencing wave propagation and sound filtering or blocking. All these aspects were carefully investigated by the authors numerically by a combination of three numerical techniques comprising the application of TD-SFEM in the case of analysis of finite and infinite computational domains, damage modelling in the case of analysis of drill-hole influence, as well as the Bloch reduction in the case of analysis of periodic computational domains. Finally, in order to back up the results of numerical simulations experimental measurements were carried out by the authors on appropriately prepared beam samples by the use of SLDV. A combined application of these numerical and experimental techniques appears to be new for that purpose and not reported in the literature available.

In that context the main objective of the paper is the demonstration of the effectiveness and accuracy of TD-SFEM as a robust and precise numerical tool for investigation of high frequency dynamic behaviour of periodic structures on the example of an isotropic Timoshenko periodic beam with drill-holes. In addition to this a parallel objective is formulated, which states that periodic structures can be successfully employed as efficient sound barriers or sound filters in the regime of high frequencies. These should be successfully confirmed experimentally by SLDV.

It should be emphasised here that numerous similarities between TD-SFEM and classical FEM result in the same modelling capabilities, which are useful in modelling structural elements of complex geometries. This also includes special elements dedicated to modelling periodic features of various types, such as drill-holes. Additionally TD-SFEM is very efficient in solving dynamic problems characterised by high frequency responses, especially wave propagation problems. This is due to its higher accuracy, when compared with classical FEM [68], resulting from the orthogonality of much higher degree approximation polynomials. Moreover, the results of numerical simulations obtained and presented in this work are backed up and verified by experimental measurements by SLDV, which additionally confirms the suitability of the approach proposed by the authors in respect of the two previously mentioned objectives of this paper.

2. Timoshenko beam spectral finite element

2.1. Element definition

All results of numerical simulations presented in this work were obtained by the use of TD-SFEM and thanks to the application of a Timoshenko beam spectral finite element with a central drill-hole, as shown in Fig. 1. The beam spectral finite element under consideration has the following dimensions: length l_e, width b and thickness h. It was also assumed that a drill-hole of diameter d was located at the centre of the element.

In the current formulation of the element the coordinates of its nodes were defined in the local coordinate system ξ as the roots of the following polynomial expression:

$$T_p^c(\xi) \equiv (1-\xi^2)U_{p-2}(\xi) = 0, \quad |\xi| \leq 1 \tag{1}$$

where $U_{p-2}(\xi)$ is a Chebyshev polynomial of the second kind and degree $p-2$, while $T_p^c(\xi)$ is a complete Chebyshev polynomial of degree p. In this case the coordinates of the element nodes ξ_i may be calculated from the relation:

$$\xi_j = -\cos\left[\frac{\pi(j-1)}{p}\right] \quad j = 1, \ldots, p+1 \tag{2}$$

On the specified set of nodes ξ_j the element shape functions can be built in the local coordinate system ξ. An interpolation function $f(\xi)$, supported on the element nodes ξ_j, can be defined in the following way:

$$f(x) = \sum_{j=1}^{p+1} N_j(\xi) f_j, \quad |x| \leq \frac{l_e}{2}, \quad \xi = \frac{2x}{l_e} \tag{3}$$

where $N_j(\xi)$ denotes one-dimensional shape functions of the element, f_j are unknown nodal values, while l_e is the element length.

MOST WIEDZY Downloaded from mostwiedzy.pl

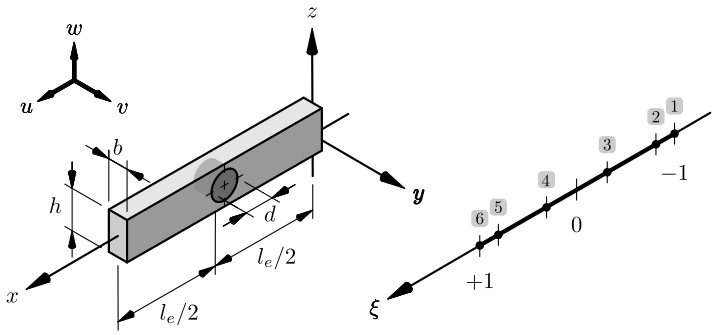

Figure 1: An isotropic Timoshenko beam spectral finite element with a central drill-hole, in the global coordinate system xyz, defined based on the fifth degree complete Chebyshev polynomials (left), the local normalised coordinate system ξ (right).

Assuming small displacements and strains within the element the displacement and strain fields of the isotropic Timoshenko beam spectral finite element under consideration can be expressed by very well–known formulae [69–71] as:

$$\begin{cases} u(x) = z\phi(x) \\ w(x) = w_0(x) \end{cases}, \quad \begin{cases} \epsilon_x = \dfrac{\partial u(x)}{\partial x} = z\dfrac{\mathrm{d}\phi(x)}{\mathrm{d}x} \\ \gamma_{xz} = \dfrac{\partial w(x)}{\partial x} + \dfrac{\partial u(x)}{\partial z} = \dfrac{\mathrm{d}w_0(x)}{\mathrm{d}x} + \phi(x) \end{cases} \tag{4}$$

where $u(x)$ and $w(x)$ denote the longitudinal and transverse element displacement components, in the global coordinate system xyz, while the independent rotation $\phi(x)$ around the y-axis as well as the transverse displacement $w_0(x)$ are nodal displacement components, defined in the element neutral axis.

Next the elemental characteristic matrices, i.e. the inertia matrix $\mathbf{M}$ and the stiffness matrix $\mathbf{K}$ can be evaluated based on the well-known and standard FEM procedures [70]:

$$\mathbf{M} = \rho \iiint_V \mathbf{N}^t \cdot \mathbf{N}\,\mathrm{d}V, \quad \mathbf{K} = \iiint_V \mathbf{B}^t \cdot \mathbf{D} \cdot \mathbf{B}\,\mathrm{d}V \tag{5}$$

where ρ is the material density, $\mathbf{D}$ is a matrix of elastic coefficients, while $\mathbf{N}$ and $\mathbf{B}$ denote the shape function and strain-displacement matrices, respectively.

2.2. Element characteristics

At this point is should be noted that numerical investigations of high frequency dynamic responses, especially including wave propagation problems, by the use of the current Timoshenko beam spectral finite element, require certain knowledge about the element performance under a very wide range of frequencies f. First of all the agreement between the applied Timoshenko beam theory and the analytical Lamb solution was tested, as presented in Fig. 2 for the ratio of the group velocity c_g to phase velocity c_p, respectively, for a non-periodic case. It was assumed that the beam under investigation was made out of aluminium of the following material properties: Young's modulus $E = 67.5$ GPa, Poisson's ratio $\nu = 0.33$ and material density $\rho = 2700$ kg/m^3 and geometrical dimensions: length $l = 1000$ mm, width $b = 10$ mm, and thickness $h = 25$ mm.

As can be seen from Fig. 2 the current Timoshenko beam theory stays in a very good agreement with the analytical solution based on the Lamb theory in the whole range of frequencies considered, i.e. for 0 Hz up to 100 kHz. It can also be seen that wave propagation signals travel within the beam as a combination of two independent wave propagation modes, known in the literature as A_0 and A_1 [71]. However, the second wave propagation mode A_1 contributes to the beam wave motion only above a certain frequency, indicated by the point A, known in the literature as a cut-off frequency, and which is equal to 61.5 kHz in the case of the analytical Lamb solution, and 62.5 kHz in the case of the current Timoshenko beam theory based

MOST WIEDZY Downloaded from mostwiedzy.pl

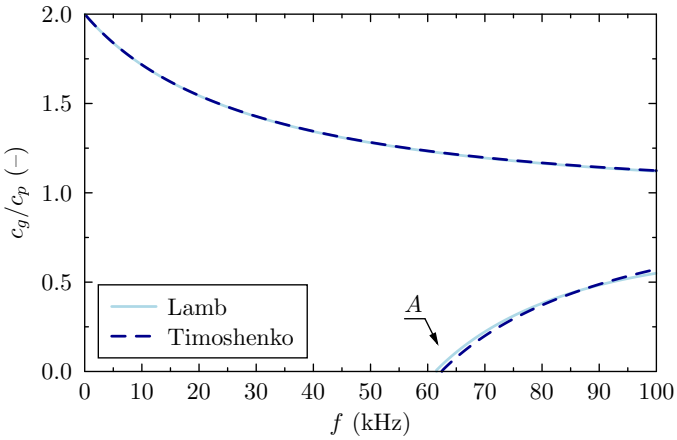

Figure 2: The ratio of the group velocity c_g to phase velocity c_p as a function of the frequency f, calculated for an aluminium beam according to the current Timoshenko beam theory and the analytical Lamb solution.

solution. Below this frequency the wave propagation mode A_1 is characterised by imaginary values of the wave number k_2. As a consequence of that it represents evanescent waves, contrary to the harmonic waves associated with the wave propagation mode A_0 and characterised by real values of the wave number k_1, as shown in Fig. 3.

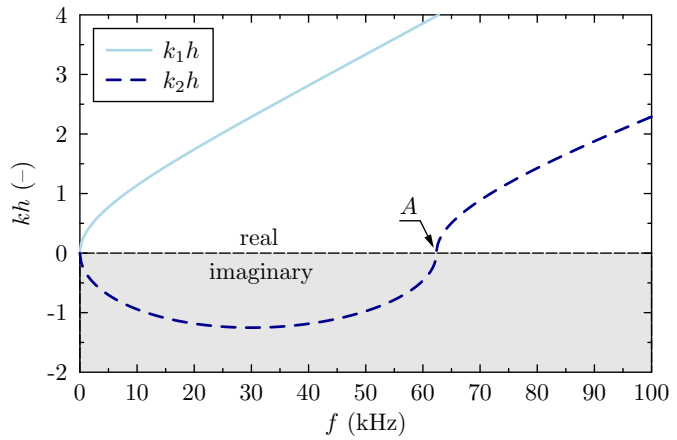

Figure 3: Non-dimensional wave number kh as a function of the frequency f, calculated for an aluminium beam according to the current Timoshenko beam theory.

The application of TD-SFEM requires the beam under investigation to be divided into a certain number n of Timoshenko beam spectral finite elements characterised by a chosen degree of approximation polynomials p. This discretisation process has a great and profound influence on calculated dynamic responses, as presented in Fig. 4 in the case of natural frequencies f_j of the beam and periodic boundary conditions. It always leads to certain discretisation errors ϵ_j resulting from the discontinuities in the stress/strain fields between spectral finite elements [68].

On the other hand it can also be considered as a source of unwanted periodicity of a beam discrete model. Its influence should be always minimalised, for example, by an increase in the degree of approximation polynomials p, as shown in Fig. 5, where vertical lines indicate multiples of the element number n. For better illustration this is also presented in Tab. 2 for the mean of the discretisation error $\bar{\epsilon}_j$ and its maximum value $\max \epsilon_j$, both calculated for the lower half of the frequency spectrum, i.e. for $j = 1, \ldots, 315$.

It can be easily noticed that the maximum values of the discretisation error $\max \epsilon_j$ are located near to,

MOST WIEDZY Downloaded from mostwiedzy.pl

or at the end of, the lower half of the frequency spectrum. For example, in the case of the approximation polynomial degree p being equal to 5 the mean value of the discretisation error $\bar{\epsilon}_j$ is 0.55% and its maximum value $\max \epsilon_j$ is 4.52%. This is associated with the natural frequency number j being equal to 298 and the natural frequency value f_j of 282.7 kHz.

Table 2: Natural frequency relative errors ϵ_j as a function of the approximation polynomial degree p, calculated based on the current formulation of a Timoshenko beam spectral finite element.

p	$\bar{\epsilon}_j$	$\max \epsilon_j$
1	4.43%	12.1% ($j = 315$, $f_j = 297.3$ kHz)
3	0.95%	4.05% ($j = 312$, $f_j = 295.8$ kHz)
5	0.55%	4.52% ($j = 298$, $f_j = 282.7$ kHz)
7	0.34%	3.16% ($j = 315$, $f_j = 297.3$ kHz)

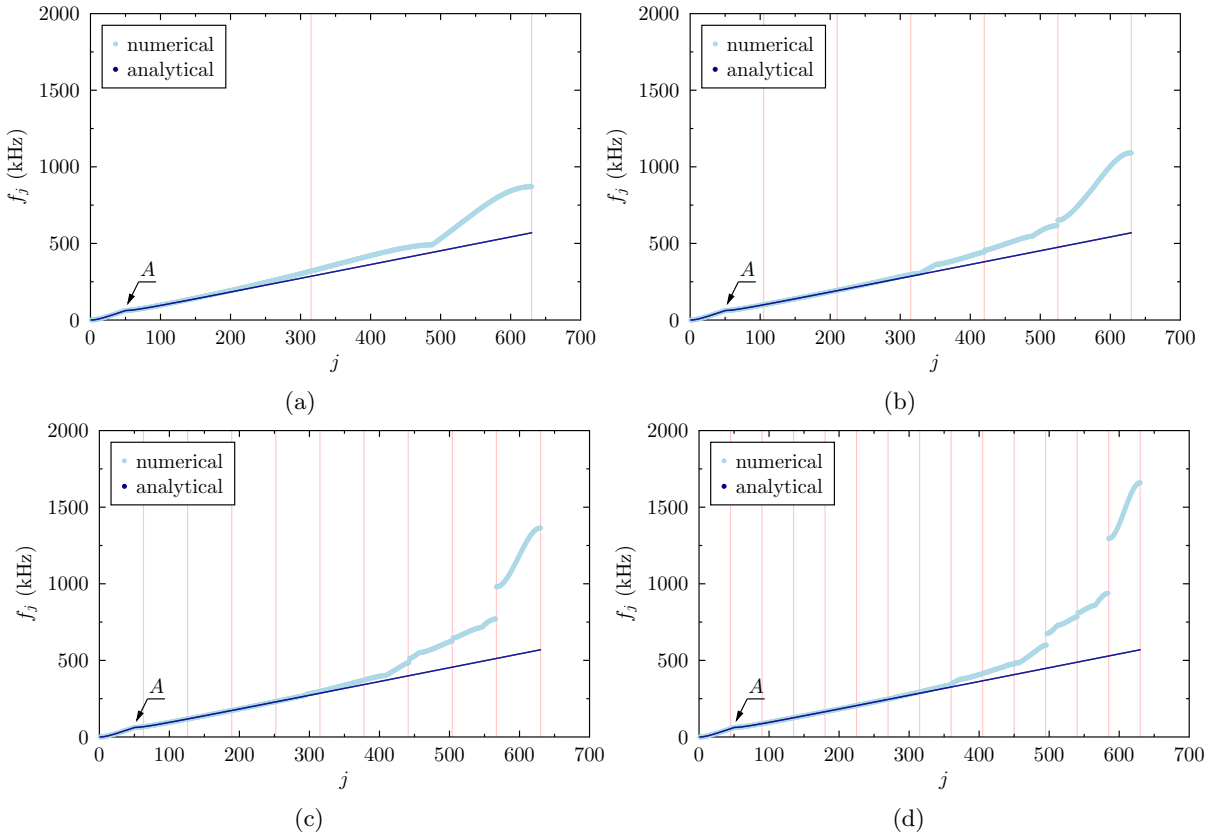

Figure 4: Frequency spectra of an aluminium beam with free ends for various degrees of approximation polynomials p and divisions into spectral finite elements n equal respectively to: $p = 1, n = 315$ (a); $p = 3, n = 105$ (b); $p = 5, n = 63$ (c) and $p = 7, n = 45$ (d). A numerical model of 632 DOFs according to the Timoshenko theory of beams [71], based on Chebyshev node distribution used for calculations by the TD-SFEM.

As shown the reduction of the discretisation error can be achieved by an appropriate selection of the approximation polynomial degree p, which in the case of TD-SFEM is usually assumed as $p = 5$. This guarantees a very high precision of the results of numerical calculations in the lower half of the frequency spectrum, which stays practically unaffected by the model periodicity due to discretisation into spectral finite elements, as seen in Fig. 5. At the same time the cost of necessary computations can be kept at an acceptable level, as the size of the elemental matrices $\mathbf{M}$ and $\mathbf{K}$ is proportional to the square of the approximation polynomial degree p. It can be clearly seen from Fig. 4 and Fig. 5 that the frequency spectra

MOST WIEDZY Downloaded from mostwiedzy.pl

exhibit certain points of strong discontinuities, known in the literature as frequency band gaps, which in the current case are entirely due to model discretisation.

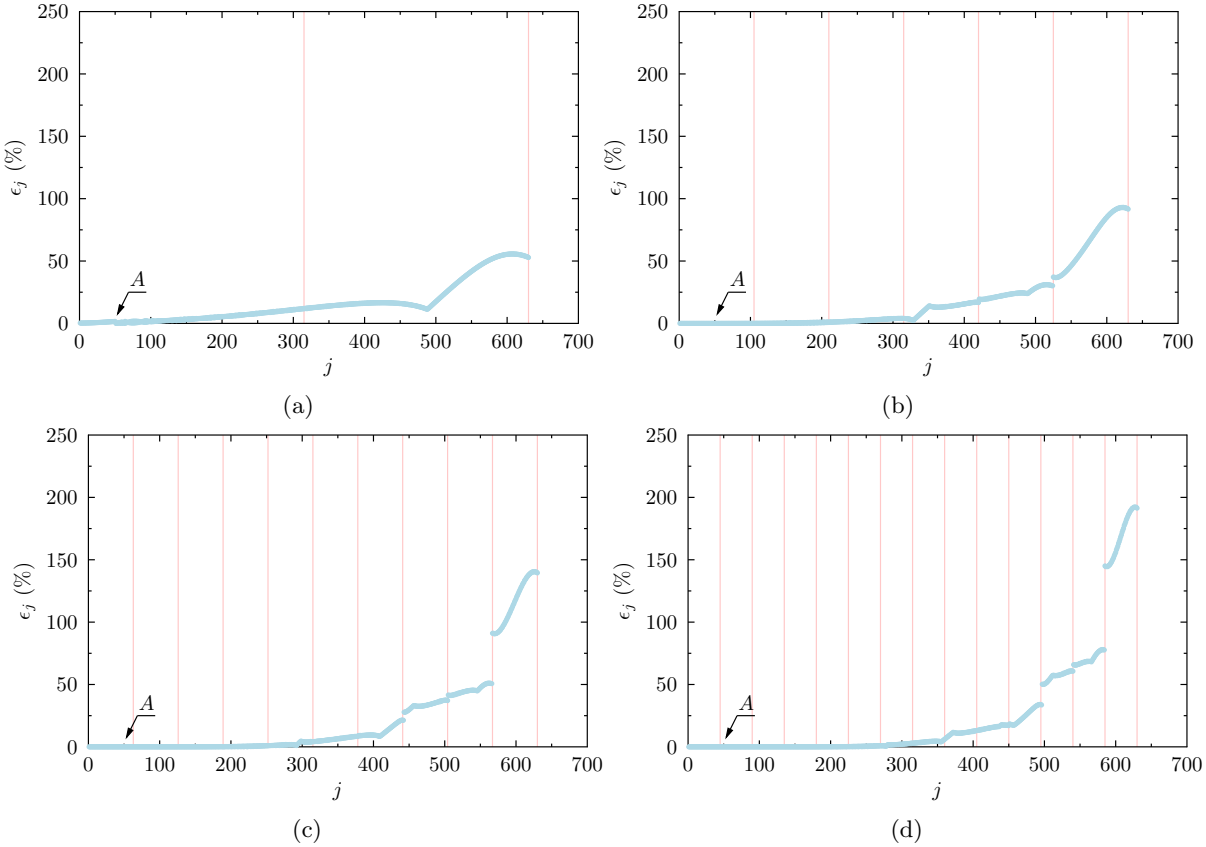

Figure 5: Relative errors of frequency spectra of an aluminium beam with free ends for various degrees of approximation polynomials p and various division into spectral finite elements n equal respectively to: $p = 1, n = 315$ (a); $p = 3, n = 105$ (b); $p = 5, n = 63$ (c) and $p = 7, n = 45$ (d). A numerical model of 632 DOFs according to the Timoshenko theory of beams [71], based on Chebyshev node distribution used for calculations by the TD-SFEM.

It should be emphasised that in the current formulation of the isotropic Timoshenko beam spectral finite element with a drill-hole, as shown in Fig. 1, the integration domain $V = V_0 - V_d$ in Eq.(5) excludes the volume of the drill hole $V_d = \pi d^2/4$, where $V_0 = bhl_e$ is the volume of the element without the drill-hole. The value of the Timoshenko shear coefficient $\kappa = 10(1+\nu)/(12+11\nu)$ has been calculated based on the formula given in [72].

Moreover, in order to take into account local stress concentrations due to the presence of the drill-hole a numerical technique based on [73–75] was employed and the matrix of elastic coefficients $\mathbf{D}$ was appropriately modified:

$$\mathbf{D} = f(\xi)\mathbf{D}_0, \quad f(\xi) = \sqrt{1-(\alpha\,\xi)^2}, \quad \xi = \frac{d}{h} \tag{6}$$

so the results of numerical simulations, obtained by the current formulation of the Timoshenko beam spectral finite element, conform well to the results of numerical calculations obtained based on a two-dimensional classical FEM model, as presented in Table. 3. The matrix of elastic coefficients that is unaffected by the presence of a drill-hole is denoted by symbol $\mathbf{D}_0$, while the value of the coefficient α in Eq. (6) was estimated numerically as equal to 1.3166.

The relative errors between the results obtained by TD-SFEM and classical FEM were calculated ac-

MOST WIEDZY Downloaded from mostwiedzy.pl

cording to the following simple metric that is based on the distance between these two sets of results:

$$\epsilon_j = \frac{|f_j - f_j^*|}{f_j^*} \times 100\%, \quad j = 1, \ldots, 10 \tag{7}$$

where $f_j (j = 1, \ldots, 10)$ are the natural frequencies of the beam calculated according to the current formulation of the isotropic Timoshenko beam spectral finite element with a drill-hole, while $f_j^* (j = 1, \ldots, 10)$ are the natural frequencies calculated by the use of the two-dimensional classical FEM model of the beam under investigation. At this point it is worth mentioning that the use of the simple metric applied by the authors should be restricted to the sets of results that are not very distinctive. In the case of very distinctive sets of results other types of metrics may be considered, as discussed in [76].

Table 3: Natural frequency relative errors $\epsilon_j (j = 1, \ldots, 10)$ as a function of the drill-hole diameter d, calculated based on the current formulation of a Timoshenko beam spectral element with a drill-hole and a two-dimensional classical FEM model.

d/h	0.00	0.08	0.16	0.24	0.32	0.40	0.48
ϵ_1	0.06%	0.13%	0.28%	0.51%	0.82%	1.25%	1.83%
ϵ_2	0.07%	0.13%	0.27%	0.49%	0.77%	1.17%	1.70%
ϵ_3	0.08%	0.13%	0.26%	0.45%	0.70%	1.04%	1.49%
ϵ_4	0.08%	0.14%	0.25%	0.40%	0.60%	0.86%	1.19%
ϵ_5	0.09%	0.14%	0.22%	0.35%	0.48%	0.65%	0.83%
ϵ_6	0.11%	0.15%	0.20%	0.28%	0.34%	0.38%	0.41%
ϵ_7	0.13%	0.15%	0.18%	0.21%	0.18%	0.09%	0.07%
ϵ_8	0.15%	0.16%	0.16%	0.12%	0.01%	0.22%	0.60%
ϵ_9	0.17%	0.17%	0.13%	0.03%	0.18%	0.56%	1.16%
ϵ_{10}	0.19%	0.18%	0.10%	0.05%	0.37%	0.92%	1.76%

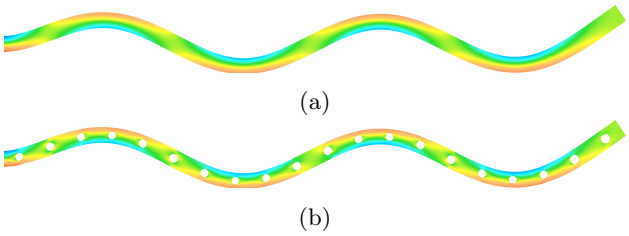

(a)

(b)

Figure 6: Distribution of bending stresses within a cantilever aluminium beam in the case of the fifth bending mode of natural vibrations. Results of numerical simulation by a two-dimensional classical FEM analysis: a beam with no drill-holes, $f_5 = 1133.25$ Hz (a); a beam with 20 evenly spaced 12 mm drill-holes along its length, $f_5 = 1153.67$ Hz (b).

The results presented in Tab. 3 refer to the case of a cantilever aluminium beam with 20 evenly spaced drill-holes along its length. The total number of degrees of freedom of the two-dimensional classical FEM model varied from 10,000 to 20,000 depending on the drill-hole diameter d, whereas the total number of degrees of freedom of the TD-SFEM model used by the authors was 600 and was independent of the drill-hole diameter d. Sample results showing the influence of the drill-holes on the distribution of bending stresses within the beam are well illustrated by Fig. 6 in the case of the fifth bending mode of natural vibrations. It can be noted that the presence of the drill-holes have relatively small impact on the distribution of bending stresses within the beam under investigation as well as the beam vibration (relative frequency shift of 1.75%) in the range of the drill-hole diameters considered.

A very good agreement can be seen between the numerical results obtained in the analysed range of natural frequencies up to 4 kHz, despite the fact that the size of the TD-SFEM numerical model used was from 16 to 32 times smaller than the reference two-dimensional FEM model. The average error is 0.43%, while its maximum value is 1.83% for the first natural frequency and the diameter of the drill-hole equal to 12 mm.

MOST WIEDZY Downloaded from mostwiedzy.pl

3. Timoshenko periodic beam

An isotropic Timoshenko periodic beam is presented in Fig. 7. It was assumed that the beam under investigation was made out of aluminium of the same material properties as specified above. It was also assumed that the source of beam structural periodicity is N evenly distributed drill-holes of diameter d placed along the beam length.

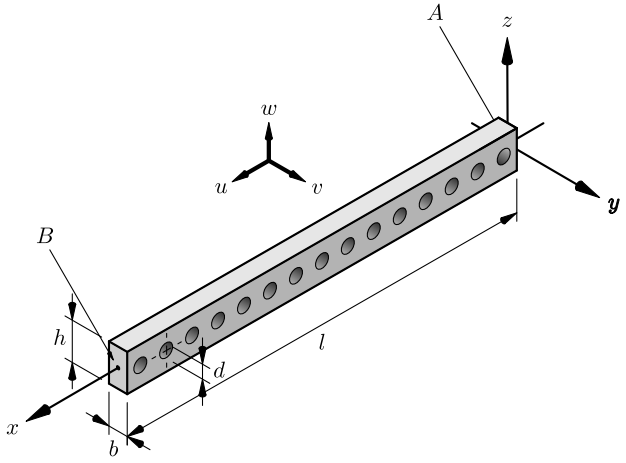

Figure 7: Geometry of a Timoshenko periodic beam with drill-holes.

3.1. Bloch theorem

The Bloch theorem is a very powerful analytical tool that enables one to study properties of various periodic structures [77, 78] in nano-, micro- as well as in macro-scales. Most commonly the Bloch theorem is used to investigate the behaviour of electrons in various crystals. However, its application is much more general. It can be successfully used to study wave-related phenomena in periodic media or structures. For example, the application of the Bloch theorem to electromagnetic waves propagating in periodic dielectric materials leads to photonic crystals, while in the case of acoustic waves in periodic media its application leads to phononic crystals [79].

The Bloch theorem states that a solution to the wave equation in a three-dimensional periodic structure $\psi(\mathbf{r})$, also known as a Bloch wave, can be represented by a combination of a plane wave $\mathrm{e}^{\mathrm{i}\mathbf{k}\cdot\mathbf{r}}$ and a periodic function $u(\mathbf{r})$:

$$\psi(\mathbf{r}) = \mathrm{e}^{\mathrm{i}\mathbf{k}\cdot\mathbf{r}} u(\mathbf{r}) \tag{8}$$

where $\mathbf{k}$ is the wave vector, $\mathbf{r}$ is the position vector within the structure, while $u(\mathbf{r})$ denotes a periodic function of the same periodicity as the periodicity of the structure.

Taking advantage of the theorem in one-dimensional case, which is the case of the Timoshenko periodic beam under consideration, it can be written that:

$$\psi(x) = \mathrm{e}^{\mathrm{i}kx} u(x) \tag{9}$$

It can be easily found that the Bloch wave $\psi(x)$ has the following property:

$$\psi(x+a) = \mathrm{e}^{\mathrm{i}k(x+a)} u(x+a) = \mathrm{e}^{\mathrm{i}ka}\mathrm{e}^{\mathrm{i}kx} u(x+a) = \mathrm{e}^{\mathrm{i}ka}\mathrm{e}^{\mathrm{i}kx} u(x) = \mathrm{e}^{\mathrm{i}ka}\psi(x) \tag{10}$$

where now k is the one-dimensional wave number, a the distance between two neighbouring cells in a one-dimensional periodic structure, which in the current case is equal to the length of a single Timoshenko beam spectral finite element l_e presented in Fig. 1.

It should be noted that Eq. (10) means that the state of motion (i.e. solution to the wave equation) within a single cell of the structure, described the Bloch wave $\phi(x)$, can be employed to describe the state

MOST WIEDZY Downloaded from mostwiedzy.pl

of motion in neighbouring cells, described by the same Bloch wave $\psi(x+a)$ with a shifted argument. This property of the Bloch wave can help to find the state of motion in each cell of the periodic structure under investigation by propagating solutions onto neighbouring cells of the structure. However, it should also be noted that the value of the upper frequency of any spectrum analysis by the application of the Bloch theorem is limited by the cell size a through its relation with the wave propagation phase velocity c_p and the maximum wave lengths k of propagating waves, i.e. $\omega = c_p k$.

Moreover, if the structure under investigation can be characterised by a certain number of cells N that are periodically placed over a distance l, so that $l = Na$, it can be written:

$$\psi(x+Na) = \psi(x) = \mathrm{e}^{\mathrm{i}kNa}\psi(x) \tag{11}$$

which requires that $\mathrm{e}^{\mathrm{i}kNa} \equiv 1$, so it can be found that:

$$k = \frac{2\pi n}{Na}, \quad n = 0, \ldots, N \tag{12}$$

This enables one to write Eq. (9) as:

$$\psi(x+a) = \mathrm{e}^{\mathrm{i}\frac{2\pi n}{N}}\psi(x) \tag{13}$$

which is essential for the application of the Bloch reduction technique that can be employed to study by the use of TD-SFEM the natural frequency spectrum of the entire beam with N evenly distributed drill-holes of diameter d placed along the beam length, as presented in Fig 7. In general, the applicability of the Bloch theorem and the Bloch reduction technique can be expanded by the superelement technique onto arbitrary shapes of three-dimensional unit cells, which is not always possible in the case of analytical investigations.

3.2. Bloch reduction

The analysis of natural vibrations of the entire beam under consideration by the use of TD-SFEM and Bloch reduction requires solution of a well-known eigenvalue problem, which can be described by the following equation:

$$(\mathbf{K} - \omega^2\mathbf{M}) \cdot \mathbf{q} = \mathbf{0} \tag{14}$$

but which is formulated at the level of a single Timoshenko beam spectral finite element with a central drill-hole. As before the symbols $\mathbf{M}$ and $\mathbf{K}$ are used to denote the elemental inertia and stiffness matrices, while $\mathbf{q}$ is a vector of nodal displacements and $\mathbf{0}$ is a corresponding null vector.

The nodal displacements of the Timoshenko beam spectral element under investigation, shown in Fig. 1, can be divided into two groups, i.e. internal nodal displacements $q_i (i = 2, \ldots, 5)$ and nodal displacements associated with element boundaries $q_i (i = 1, 6)$:

$$\mathbf{q} = \{q_1, q_2, q_3, q_4, q_5, q_6\}, \quad q_j = (w_j, \phi_j), \quad j = 1, \ldots, 6 \tag{15}$$

where w_j and ϕ_j represent two nodal degrees of freedom of the element.

Thanks to the application of the Bloch theorem the size of the eigenvalue problem associated with the analysis of natural vibrations of the entire Timoshenko periodic beam can be reduced to repeated solution of the eigenvalue problem defined at the level of a single Timoshenko spectral finite element by the use of the following relation for boundary nodal displacements q_1 and q_6:

$$q_6 = q_1 \mathrm{e}^{\mathrm{i}\frac{2\pi n}{N}}, \quad n = 0, \ldots, N \tag{16}$$

In this manner the size of the original eigenvalue problem (14) can be reduced to:

$$[\mathbf{K}_r(n) - \omega^2\mathbf{M}_r(n)] \cdot \mathbf{q}_r(n) = \mathbf{0}, \quad n = 0, \ldots, N \tag{17}$$

where now:

$$\begin{aligned} \mathbf{K}_r(n) &= \mathbf{A}^t(n) \cdot \mathbf{K} \cdot \mathbf{A}(n) \\ \mathbf{M}_r(n) &= \mathbf{A}^t(n) \cdot \mathbf{M} \cdot \mathbf{A}(n) \end{aligned} \tag{18}$$

MOST WIEDZY Downloaded from mostwiedzy.pl

are reduced elemental stiffness and inertia characteristic matrices, respectively.

The non-zero elements of the rectangular matrix $\mathbf{A}(n)$ of size 12×10 can be defined in the following manner:

$$\begin{aligned} A_{j,j} &= 1, \qquad j = 1, \ldots, 10 \\ A_{j,1} &= \mathrm{e}^{\mathrm{i}\frac{2\pi n}{N}}, \qquad j = 11, 12 \end{aligned} \tag{19}$$

4. Results of numerical simulations

4.1. Natural frequency spectrum

Firstly the influence of the drill-hole diameter d on the natural frequencies f_j of the beam under consideration was investigated, where as before j is the natural frequency number. In this study the first 120 natural frequencies of the beam were analysed for 4 different numbers of the drill-holes N, these being: 50, 40, 30 and 20. It was assumed that the beam was modelled by Timoshenko beam spectral finite elements based on the fifth degree complete Chebyshev polynomials. The total number of degrees of freedom of the numerical model was constant and equal to 10. The periodic boundary conditions were used in this case.

In Fig. 8 results of numerical simulations are presented calculated for the relative drill-hole diameter $d/h = 0.5$ and the number of drill-holes $N = 50$. They were obtained based on the Bloch reduction technique and the use of a single isotropic Timoshenko beam spectral finite element with a central drill-hole, as previously discussed.

It should be remembered that the properties of the numerical model itself, resulting from the assumed discretisation technique by TD-SFEM, are an additional source of frequency band gaps that dominate in the upper half of the calculated frequency spectrum [68]. These frequency band gaps can effectively mask the influence of the drill-holes being the primary and assumed source of beam periodicity, as shown in Fig. 4. For that reason only the lower half of the calculated frequency spectrum is considered as consisting of valuable information about the influence of the periodicity from the presence of drill-holes in the range of the relative drill-hole diameters d/h from 0 to 0.5.

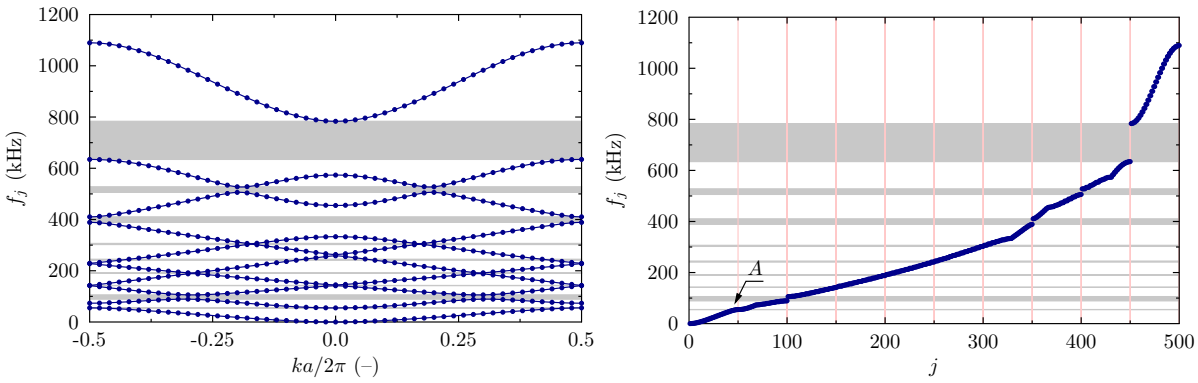

Figure 8: Natural frequency spectrum of an aluminium Timoshenko periodic beam as a function of: relative wave number $ka/2\pi$ (a), natural frequency number j (b). Results obtained based on the Bloch reduction technique and the application of an isotropic Timoshenko beam spectral finite element with a central drill-hole for the relative drill-hole diameter $d/h = 0.5$ and the number of drill-holes $N = 50$.

It can be seen from Fig. 8 that the appearance of the drill-holes results in the presence of frequency band gaps in the lower half of the frequency spectrum. Moreover, as before the frequency band gaps present appear in the calculated frequency spectrum of the beam at frequency numbers j being multiples of the number of drill-holes N. This is clearly visible in Fig. 8, when the spectrum is presented just as a function of the natural frequency number j.

MOST WIEDZY Downloaded from mostwiedzy.pl

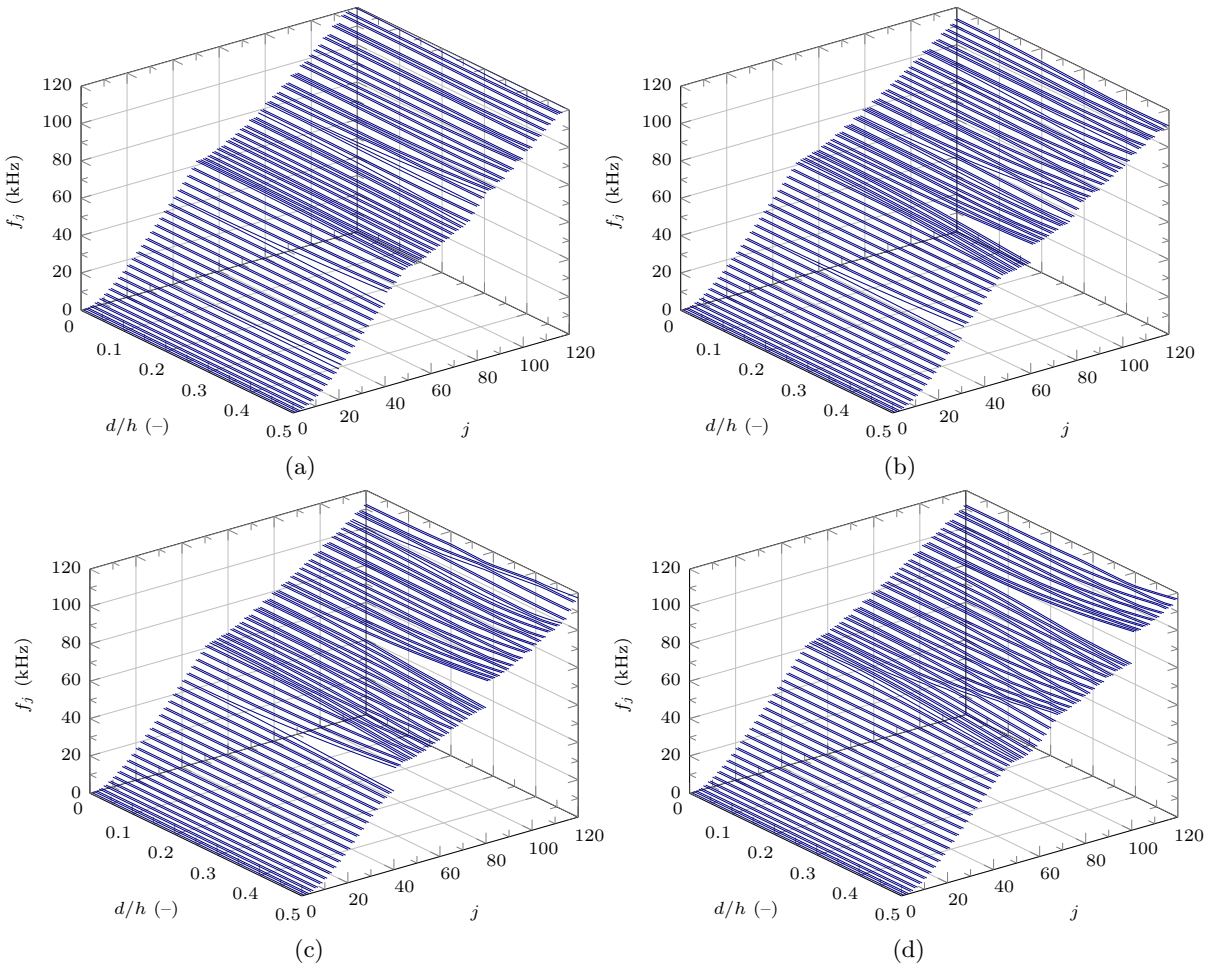

Figure 9: The influence of the relative drill-hole diameter d/h on natural frequencies f_j of an aluminium Timoshenko periodic beam for various numbers of drill-holes N equal respectively to: $N = 20$ (a), $N = 30$ (b), $N = 40$ (c) and $N = 50$ (d). Results of numerical calculations based on the Bloch reduction technique and the use of a single isotropic Timoshenko beam spectral finite element with a central drill-hole.

The influence of the relative drill-hole diameter d/h and the number of drill-holes N is presented in Fig. 9. Similarly, the results of numerical simulations were calculated based on the Bloch reduction technique and the use of a single isotropic Timoshenko beam spectral finite element with a central drill-hole.

It can be seen from Fig. 9 that an increase in the relative drill-hole diameter d/h results in an increase in the widths of the frequency band gaps observed $\Delta f_m (m = 1, \ldots, 9)$. For small relative drill-hole diameters $d/h < 0.25$ the widths of the frequency band gaps Δf_m stay comparable to the distance between two neighbouring natural frequencies of the beam. On the other hand for higher beam periodicities N/l , i.e. for greater number of drill-holes N, the widths of frequency band gaps Δf_m increase in comparison to smaller numbers of drill-holes N. However, they also move towards higher natural frequencies f_j and/or higher frequency numbers j in close correlation with the number of drill-holes N.

4.2. Propagation of elastic waves

Next the wave propagation phenomena in the beam under consideration was investigated. The main purpose of this investigation was to demonstrate the usefulness of periodic structures as sound filters or sound barriers as well as the effectiveness of the application of TD-SFEM. In order to do that it was assumed that a transverse displacement time signal $w(t)$, due to a unit force excitation applied at point A in the form of

MOST WIEDZY Downloaded from mostwiedzy.pl

Table 4: Frequency band gaps Δf_m in the natural frequency spectrum of an aluminium Timoshenko periodic beam. Results obtained based on the Bloch reduction technique and the application of an isotropic Timoshenko beam spectral finite element with a central drill-hole for the relative drill-hole diameter $d/h = 0.5$ and the number of drill-holes $N = 50$.

m	$\Delta f_m = f_{Nm+1} - f_{Nm}$	f_{Nm}	f_{Nm+1}
1	0.1 kHz	55.0 kHz	55.1 kHz
2	16.8 kHz	89.1 kHz	105.9 kHz
3	0.8 kHz	141.9 kHz	142.7 kHz
4	4.0 kHz	187.9 kHz	191.9 kHz
5	4.0 kHz	241.0 kHz	245.0 kHz
6	4.4 kHz	302.3 kHz	306.7 kHz
7	21.6 kHz	388.8 kHz	410.4 kHz
8	21.9 kHz	505.9 kHz	527.8 kHz
9	148.9 kHz	634.5 kHz	783.4 kHz

20 sine pulses of carrier frequency f_c, modulated by the Hann window, propagates within the beam from point $A(x = 0)$ to point $B(x = l)$, as shown in Fig. 7. Time histories $w(t)$ and amplitude spectra $a(\omega)$ of those signals, based on the results of numerical simulations by TD-SFEM, were calculated at point B for the relative diameter of drill-holes $d/h = 0.5$.

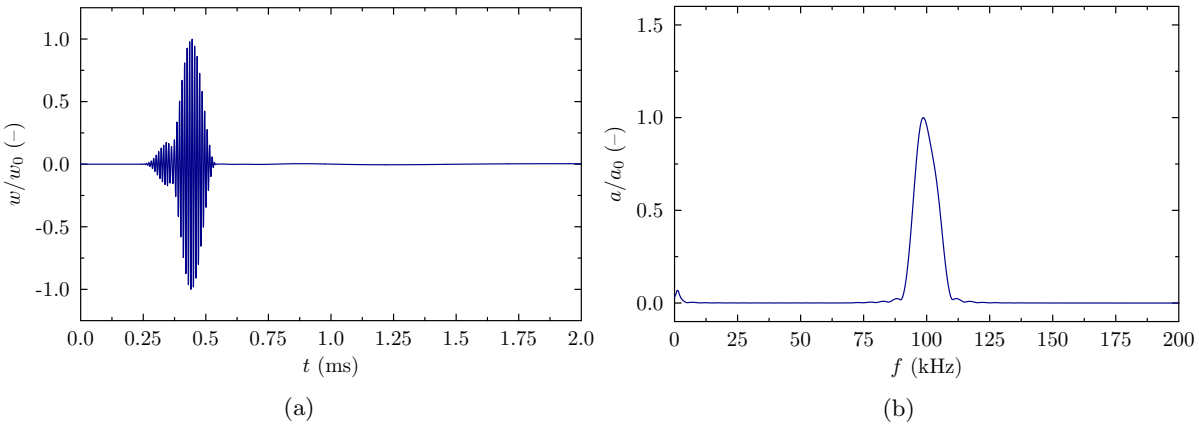

Figure 10: Time history (a) and amplitude spectrum (b) of propagating elastic waves in an aluminium Timoshenko non-periodic beam for the excitation signal carrier frequency $f_c = 100$ kHz. Results obtained based on TD-SFEM and the application of an isotropic Timoshenko beam spectral finite element with a central drill-hole for the relative drill-hole diameter $d/h = 0.0$.

In order to remove any artefacts from back-reflected signals at point B that could influence the results of numerical calculations due to the finite simulation time T as well as no material damping in the numerical model, it was additionally assumed that the length l represents a section of an infinite periodic beam of the same periodicity N/l and intensity d/h.

According to [80] the remaining infinite part of the beam was modelled by a so-called through-off structural element [81] defined in the time domain, for which length l_a and wave attenuation properties s and p had to be adjusted to the length of the longest waves propagating within the beam. Based on the results presented in [80] the following values of the adjustable parameters were used: length $l_a = 1000$ mm, $s = 7$ and $p = 3$. As a consequence of that the whole numerical model consisted of 100 isotropic Timoshenko beam spectral finite elements with central drill-holes, which resulted in 1000 degrees of freedom in total. For solving the equation of motion in time the Newmark method was employed with no artificial numerical damping ($\alpha = 0.25, \delta = 0.5$), while the simulation time $T = 2$ ms was divided into 2^{12} time steps. The free type of boundary conditions was used now. For calculation of signal amplitude spectra the discrete fast Fourier transform (DFFT) was employed.

The results obtained are presented in Figs. 10–13 as normalised signal time histories as well as normalised amplitude signal spectra. In each case the normalisation of the signal under consideration, i.e. time history

MOST WIEDZY Downloaded from mostwiedzy.pl

$w(t)$ or amplitude spectrum $a(\omega)$, was performed based on the maximum value of an appropriate reference signal $w_0(t)$ and $a_0(\omega)$ obtained in the case of the non-periodic beam, i.e. when the relative diameter of drill-holes $d/h = 0$.

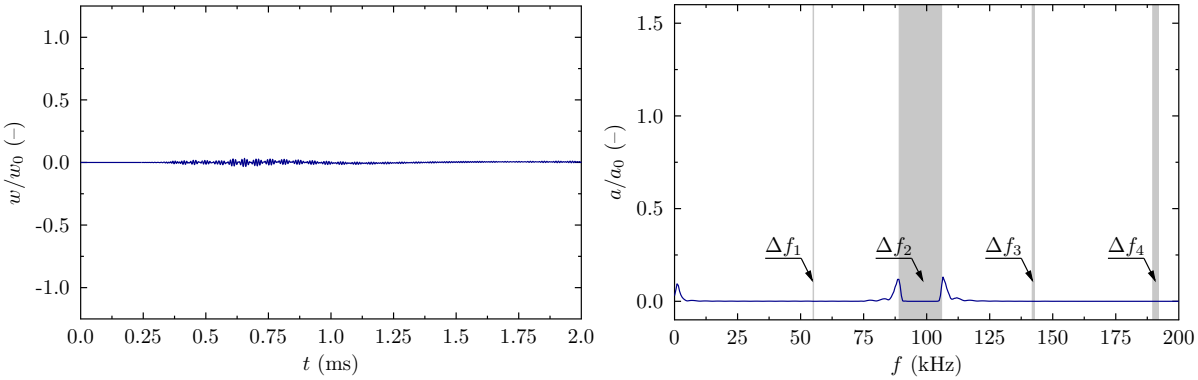

Figure 11: Time history (a) and amplitude spectrum (b) of propagating elastic waves in an aluminium Timoshenko periodic beam for the excitation signal carrier frequency $f_c = 100$ kHz. Results obtained based on TD-SFEM and the application of an isotropic Timoshenko beam spectral finite element with a central drill-hole for the relative drill-hole diameter $d/h = 0.5$ and the number of drill-holes $N = 50$.

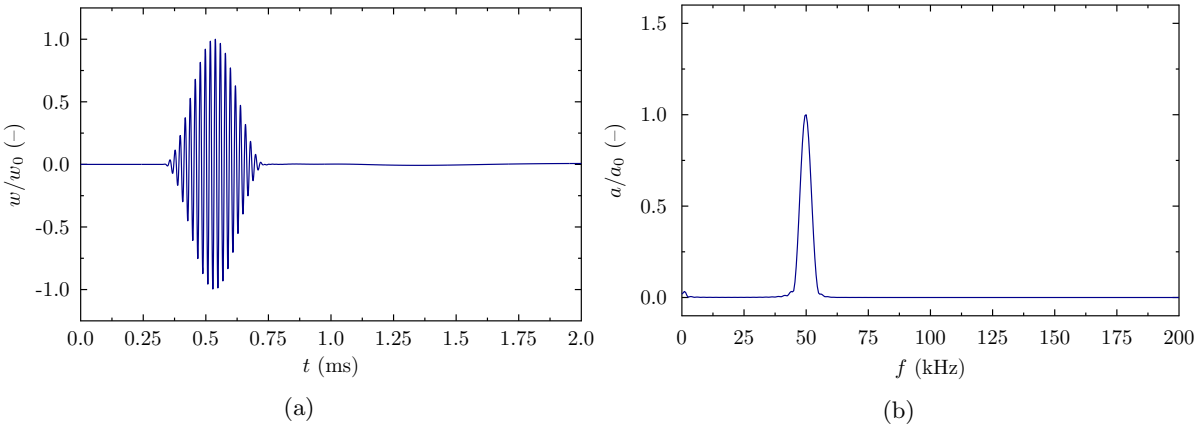

Figure 12: Time history (a) and amplitude spectrum (b) of propagating elastic waves in an aluminium Timoshenko non-periodic beam for the excitation signal carrier frequency $f_c = 50$ kHz. Results obtained based on TD-SFEM and the application of an isotropic Timoshenko beam spectral finite element with a central drill-hole for the relative drill-hole diameter $d/h = 0.0$.

It is evident from the results presented in Figs. 10–13 that attenuation properties of the beam under consideration have their source in the presence of frequency band gaps $\Delta f_m (m = 1, \ldots, 9)$ in its spectrum. In a non-periodic case, regardless of the carrier frequency f_c of the excitation, signals propagate within the beam freely as two modes, as seen in Fig. 10, or a single mode, as seen in Fig. 12. The only changes observed in the form of these signals are due to the dispersive nature of propagating elastic waves [71]. However, in a periodic case, for signals for which a significant part of their frequency content falls within frequency band gaps, a considerable decrease in the time signal amplitude is observed, as seen in Fig. 11, both in the time and frequency domains. In the time domain the signal is attenuated to 3.1% of its initial maximum value, while in the frequency domain the signal is attenuated to 13% of its initial maximum value.

Contrary to that, for signals for which their frequency content falls outside frequency band gaps, signal strengthening can be noticed. This manifests in a considerable increase in the time signal amplitude, as seen

MOST WIEDZY Downloaded from mostwiedzy.pl

in Fig. 13. In the time domain the signal is amplified to 117% of its initial maximum value, while in the frequency domain the signal is amplified to 149% of its initial maximum value. The signal strengthening, i.e. signal amplification, is a direct consequence of a decrease in the structural stiffness $\mathbf{K}$ of the beam due to the presence of the drill-holes. This effect can be effectively compensated for, only for the signals for which a significant part of their frequency content falls within frequency band gaps, present in the frequency spectrum of the beam.

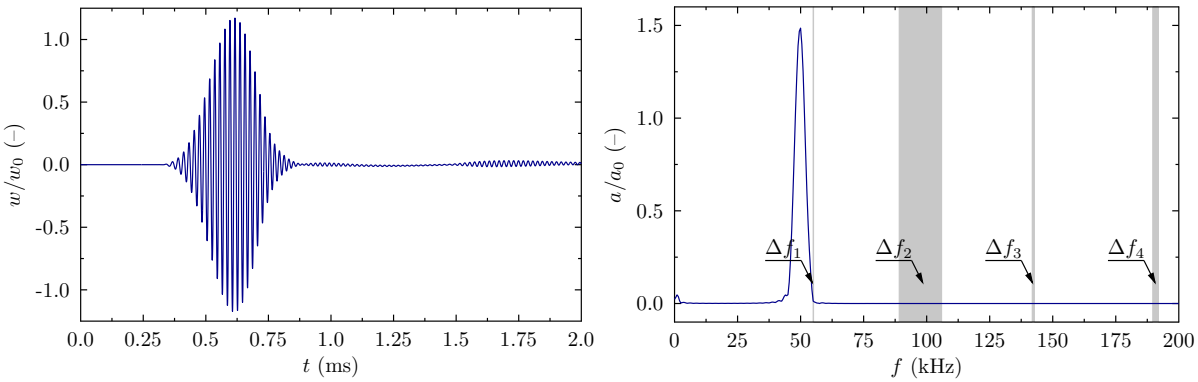

Figure 13: Time history (a) and amplitude spectrum (b) of propagating elastic waves in an aluminium Timoshenko periodic beam for the excitation signal carrier frequency $f_c = 50$ kHz. Results obtained based on TD-SFEM and the application of an isotropic Timoshenko beam spectral finite element with a central drill-hole for the relative drill-hole diameter $d/h = 0.5$ and the number of drill-holes $N = 50$.

5. Experimental measurements

High frequency dynamic responses of aluminium periodic beams with drill-holes were investigated by the authors experimentally by the use of the Scanning Laser Doppler Vibrometry (SLDV). The main element of the test rig used for that purpose was a one-dimensional Doppler laser scanning vibrometer, Polytec model PSV-400, as well as an anti-vibration table. The rig was additionally equipped with a linear amplifier, American Piezo, Inc.model EPA-140 (±200 Vpp). In the experiments American Piezo, Inc. PZT-850 disc (10 mm ×10 mm) transducers were used to excite the beams in a wide range of frequencies. Experimental measurements were carried out on nine aluminium beams of the following dimensions: length $L = 1.2$ m, height $a = 25$ mm and width $b = 10$ mm.

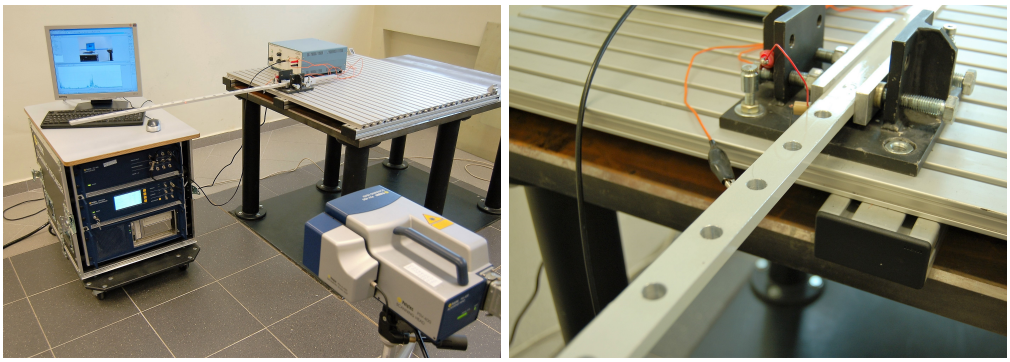

(a) (b)

Figure 14: A view of the 1-D Doppler scanning laser vibrometer unit (a) and a tested beam sample (b).

MOST WIEDZY Downloaded from mostwiedzy.pl

In order to conform to the results of numerical calculations by TD-SFEM, in the case of eight beams the source of their periodicity was assumed to be $N = 20$ cylindrical drill-holes. The diameter of drill-holes d varied from 5 mm up to 12 mm, while the drill-holes were equally spaced along the length $L = 1000$ mm with a 200 mm margin on one side. As previously the influence of the relative diameter d/h of drill-holes on beam dynamics was taken into consideration. Both their natural frequency spectra as well as the propagation of guided elastic waves were carefully investigated by the authors.

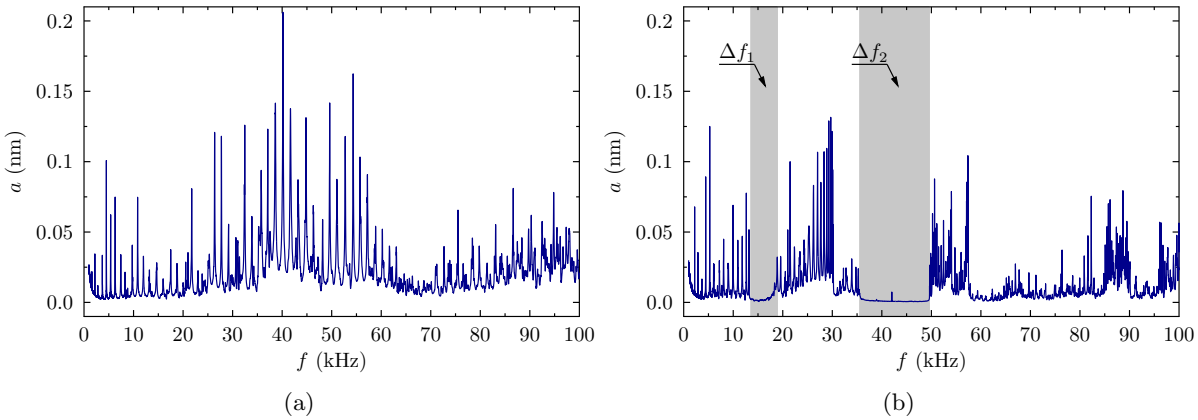

Figure 15: Amplitudes of natural frequencies of an aluminium cantilever Timoshenko beam: non-periodic (a), periodic (b), for chirp excitation obtained experimentally by the use of 1-D SLDV. In the case of the periodic beam results obtained for the relative drill-hole diameter $d/h = 0.5$ and the number of drill-holes $N = 20$.

Initially amplitudes of natural frequencies of the beams were tested. The chirp type of excitation was used for that purpose within the frequency range from 1 kHz up to 200 kHz, covering 200 equally spaced frequency points. In this case the cantilever type of boundary conditions was assumed and therefore the effective length of the beams was reduced to $l = 1000$ mm due to 200 mm of clamping. Dynamic displacement responses were measured consecutively in 2^{11} points, equally spaced along the beam lengths, i.e. on top or bottom/side, as shown in Fig. 7, and which next were averaged for each frequency point. For every beam a single measurement for each frequency point was $T = 12.8$ ms, while the total measurement time was $2^{11} \times 12.8$ ms $= 26.2$ s. Sample results of experimental measurements obtained in this way are presented in Fig. 15.

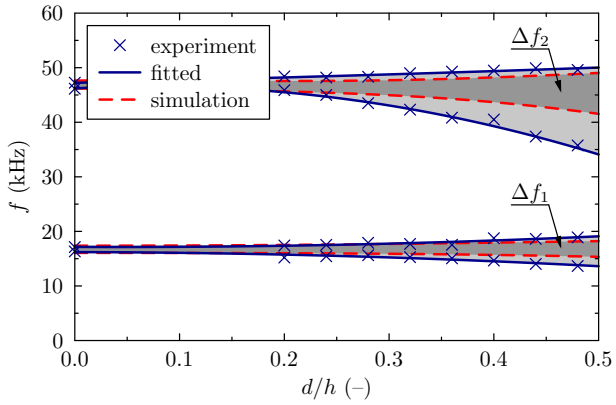

Figure 16: Comparison of experimentally measured and numerically calculated frequency band gaps within the natural frequency spectrum of an aluminium cantilever Timoshenko periodic beam as a function of the relative drill-hole diameter d/h. Results obtained for the number of drill-holes $N = 20$.

Thanks to the programme of experimental measurements carried out it was possible to identify the widths

MOST WIEDZY Downloaded from mostwiedzy.pl

of frequency band gaps resulting from the presence of the drill-holes. In the case of the beams tested there were two frequency band gaps that could be easily observed within the investigated range of frequencies, as shown in Fig. 15. Based on the measurements carried out on all aluminium beams the influence of the relative drill-hole diameter d/h on the widths of frequency band gaps in the natural frequency spectrum of the beams could be investigated.

The result of this investigation is presented in Fig. 16 as a comparison of numerical and experimental analyses. It can be seen from Fig. 16 that the results of experimental measurements by one-dimensional SLDV correspond well to the results of numerical simulations by TD-SFEM in terms of the position of the middle of frequency band gaps within the frequency spectrum of the beam. However, the widths of the frequency band gaps are underestimated in the case of TD-SFEM. This can result from underestimation of the correction function $f(\xi)$ in Eq. (6) that possibly should be based on higher natural frequencies, rather than first ten natural frequencies, in order to take into account a very localised influence of stress concentration effects for higher modes of natural vibrations. An alternative can be a correction function $f(\xi)$ entirely based on the results of experimental measurements.

Next, propagation of guided elastic waves was investigated, based on the results obtained from previous measurements related to the natural frequency spectra. Two carrier frequencies $f_c = 44$ kHz and $f_c = 22$ kHz were chosen for that purpose in order to demonstrate the effectiveness of signal filtering capabilities of the periodic beam under investigation.

In both cases the signals had the same form of 10 sine pulses modulated by the Hann window. The duration of excitation was $T = 12.8$ ms, while that time was uniformly sampled in 2^{15} points. As easily seen from Fig. 16 the higher carrier frequency $f_c = 44$ kHz falls in the middle of the upper frequency band gap Δf_2, while the lower carrier frequency $f_c = 22$ kHz stays slightly above the lower frequency band gap Δf_2. Therefore strong signal attenuation is expected to be observed in the case of the higher carrier frequency of 44 kHz rather than in the case of the lower carrier frequency of 22 kHz. All experimental measurements were carried out for the free type of boundary conditions. As a consequence the effective length of the beam was equal to $l = 1200$ mm. In this case the non-periodic part of each beam of 200 mm was used as an auxiliary zone providing enough space for full signal development.

The result of this investigation is presented in Fig. 17. As expected for the higher carrier frequency of 44 kHz falling in the middle of the upper frequency band gap Δf_2, strong signal attenuation is observed with its average value of 91.5% in the initial 1.55 ms. This behaviour is not present for the lower carrier frequency of 22 kHz, which stays above the neighbouring frequency band gap Δf_1, where no apparent attenuation of the propagating signal is visible.

6. Conclusions

The results of numerical calculations by TD-SFEM, as well as experimental measurements by one-dimensional SLDV presented in this work and related with the high frequency dynamics of an aluminium Timoshenko periodic beam, allow the authors to formulate the following general conclusions:

1. The structural periodicity of the Timoshenko beam under investigation is a direct consequence of the presence of evenly distributed drill-holes along its length.
2. The structural periodicity, expressed by the number of drill-holes per unit length, has a profound influence on the beam dynamic behaviour, which manifests itself in the presence of frequency band gaps in the beam natural frequency spectrum.
3. The intensity of the periodicity, expressed by the relative diameter of drill-holes, can be easily tuned by increasing the diameter of the drill-holes, while the periodicity itself can be modified by increasing the number of the drill holes.
4. For the same intensities of periodicity, as well as for higher periodicities, the number of frequency band gaps is smaller, but their widths in the frequency domain increase.
5. For the same periodicities and for their higher intensities the widths of frequency band gaps also increase.

MOST WIEDZY Downloaded from mostwiedzy.pl

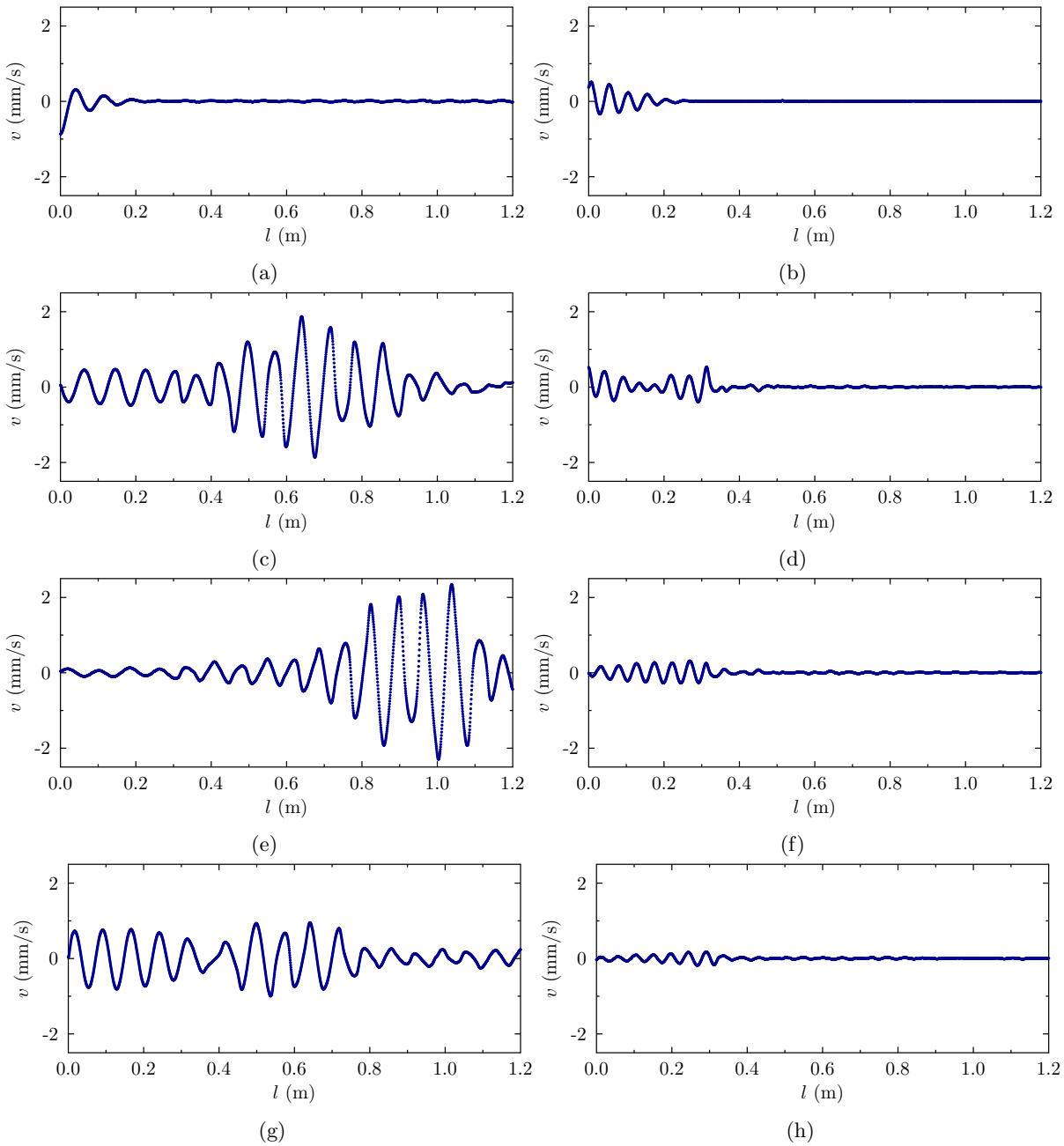

Figure 17: Time histories of propagating elastic waves in an aluminium Timoshenko periodic beam for the excitation signal carrier frequencies $f_c = 22$ kHz (left) and $f_c = 44$ kHz (right) at time instances: $t = 0.20$ ms (a–b), $t = 0.65$ ms (c–d), $t = 1.10$ ms (e–f) and $t = 1.65$ ms (g–h). Results obtained based experimentally by the use of 1D-SLDV for the relative drill-hole diameter $d/h = 0.5$ and the number of drill-holes $N = 20$.

MOST WIEDZY Downloaded from mostwiedzy.pl

6. Low values of the structural periodicity define the boundary between periodic and non-periodic structures.
7. For the Timoshenko beam under investigation this boundary was 20 drill-holes along the beam length. In such cases the differences between subsequent natural frequencies of the beam are of similar magnitudes as expected frequency band gaps.
8. For higher values of the structural periodicity the influence of non-periodic boundary conditions becomes smaller with the increase in the structural periodicity. In such cases the results of numerical calculations by TD-SFEM, for a full numerical model, tend to the results of numerical calculations obtained for a single unit cell and periodic type of boundary conditions.
9. The structural periodicity can be employed as an effective means to attenuate or filter out signals propagating within an isotropic Timoshenko beam.
10. The effectiveness of this process depends on the correlation between the signal frequency content and the beam periodic properties, expressed by periodicity and the intensity of periodicity, thus influencing its dynamic properties.
11. TD-SFEM is an extremely effective numerical tool that can be used to study wave propagation phenomena in periodic structures numerically, while as its experimental counterpart 1D-SLDV can be used.
12. The effectiveness of numerical investigations by TD-SFEM can be additionally increased by the application of the Bloch theorem and the Bloch reduction technique, which greatly helps to reduce the size of numerical models as well as the time of necessary computations limiting these models to numerical models of a single unit cell.
13. The applicability of the Bloch theorem and the Bloch reduction technique can be additionally enhanced by TD-SFEM and the superelement technique onto arbitrary shapes of three-dimensional unit cells, which is not possible in the case of analytical investigations.
14. The application of TD-SFEM in the case of problems involving high frequency dynamic responses must always be preceded by careful investigation of periodic properties of the numerical model used. This helps to minimise the negative influence of numerical model periodic properties that can effectively mask or distort results of numerical calculations.
15. In general, only the lower half of the frequency spectra remains unaffected by periodic properties of the numerical model used. For this reason only this part of the frequency spectra should be considered as providing valuable information about the dynamic responses of periodic structures under investigation. The upper half of the frequency spectra can be disregarded, as a strong influence of periodic properties of the numerical models reveals there and dominates calculated dynamic responses.
16. Alternatively, in the case of problems involving high frequency dynamic responses periodic properties of numerical models can be restrained by enforcing the continuity of the displacement fields as well as its derivatives between neighbouring finite elements. For example, this is possible through the application of quintic Hermite splines instead of Chebyshev polynomials as elemental approximation polynomials.

7. Acknowledgements

The authors of this work would like to gratefully acknowledge the support for their research provided by the National Science Centre via project UMO-2012/07/B/ST8/03741 *Wave propagation in periodic structures*. All results presented in this paper have been obtained by the use of the software available at the Academic Computer Centre in Gdansk in the frame of a computational project.

References

[1] R. Liu, C. Ji, J. J. Mock, J. Y. Chin, T. J. Cui, D. R. Smith, Broadband ground-plane cloak, Science 323 (2009) 366–369.
[2] N. Kundtz, D. R. Smith, Extreme-angle broadband metamaterial lens, Nature Materials 9 (2010) 129–132.
[3] C. M. Soukoulis, M. Wegener, Past achievements and future challenges in the development of three-dimensional photonic metamaterials, Nature Photonics 5 (2011) 523–530.

MOST WIEDZY Downloaded from mostwiedzy.pl

[4] J. Li, C. T. Chan, Double-negative acoustic metamaterial, Physical Review E 70 (2004) 055602.
[5] S. Zhang, L. Yin, N. Fang, Focusing ultrasound with an acoustic metamaterial network, Physical Review Letters 102 (2009) 194301.
[6] T. Chen, Y.-L. Tsai, A derivation for the acoustic material parameters in transformation domains, Journal of Sound and Vibration 332 (2013) 766–779.
[7] X. D. Zhang, Z. Y. Liu, Negative refraction of acoustic waves in two-dimensional phononic crystals, Applied Physics Letters 85 (2004) 341–343.
[8] M. Ricci, X. Hua, R. Prozorov, A. P. Zhuravel, A. V. Ustinov, S. M. Anlage, Tunability of superconducting metamaterials, IEEE Transactions on Applied Superconductivity 17 (2007) 918–921.
[9] S. M. Anlage, The physics and applications of superconducting metamaterials, Journal of Optics 13 (2011) 024001.
[10] P. Tassin, T. Koschny, M. Kafesaki, C. M. Soukoulis, A comparison of graphene, superconductors and metals as conductors for metamaterials and plasmonics, Nature Photonics 6 (2012) 259–264.
[11] Y. Ding, Z. Liu, C. Qiu, J. Shi, Metamaterial with simultaneously negative bulk modulus and mass density, Physical Review Letters 99 (2007) 093904.
[12] H. H. Huang, C. T. Sun, Theoretical investigation of the behavior of an acoustic metamaterial with extreme Young's modulus, Journal of the Mechanics and Physics of Solids 59 (2011) 2070–2081.
[13] H. H. Huang, C. T. Sun, Anomalous wave propagation in a one-dimensional acoustic metamaterial having simultaneously negative mass density and Young's modulus, Journal of the Acoustical Society of America 132 (2012) 2887–2895.
[14] M. M. Sigalas, E. N. Economou, Elastic and acoustic wave band structure, Journal of Sound and Vibration 158 (1992) 377–382.
[15] M. S. Kushwaha, P. Halevi, L. Dobrzyński, B. Djafari-Rouhani, Acoustic band structure of periodic elastic composites, Physical Review Letters 71 (1993) 2022–2025.
[16] M. M. Sigalas, E. Economou, Elastic waves in plates with periodically placed inclusions, Journal of Applied Physics 75 (1994) 2845–2850.
[17] I. E. Psarobas, N. Stefanou, A. Modinos, Scattering of elastic waves by periodic arrays of spherical bodies, Physical Review B 62 (2000) 278–291.
[18] M. M. Sigalas, N. García, Theoretical study of three dimensional elastic band gaps with the finite-difference time-domain method, Journal of Applied Physics 87 (2000) 3122–3125.
[19] R. K. Narisetti, M. J. Leamy, M. Ruzzene, A perturbation approach for predicting wave propagation in one-dimensional nonlinear periodic structures, Journal of Vibration and Acoustics 132 (2010) 031001.
[20] A. Żak, M. Krawczuk, Ł. Doliński, Dynamics of 1-D periodic structures. Numerical and experimental investigation, The 21st International Congress on Sound and Vibration, 13-17 July 2014, Beijing, China (2014) 1–8.
[21] A. Żak, M. Krawczuk, W. Waszkowiak, Longitudinal, torsional and flexural dynamics of 1-D periodic structures, The 22st International Congress on Sound and Vibration, 12-16 July 2015, Florence, Italy (2015) 1–8.
[22] D. J. Mead, Wave propagation in continuous periodic structures: Research contribution from Southampton, 1964–1995, Journal of Sound and Vibration 190 (1996) 495–524.
[23] R. S. Langley, The response of two-dimensional periodic structures to point harmonic forcing, Journal of Sound and Vibration 197 (1996) 447–469.
[24] D. Bigoni, M. Gei, A. B. Movchan, Dynamics of a prestressed stiff layer on an elastic half space: filtering and band gap characteristics of periodic structural models derived from long-wave asymptotics, Journal of the Mechanics and Physics of Solids 56 (2008) 2494–2520.
[25] Y. Lu, J. Guo, Band gap of strained graphene nanoribbons, Nano Research 3 (2010) 189–199.
[26] H. J. Xiang, Z. F. Shi, S. J. Wang, Y. L. Mo, Periodic materials-based vibration attenuation in layered foundations: Experimental validation, Smart Materials and Structures 21 (2012) doi:10.1088/0964–1726/21/11/112003.
[27] Y. Xiao, J. Wen, D. Yu, X. Wen, Flexural wave propagation in beams with periodically attached vibration absorbers: Band-gap behavior and band formation mechanisms, Journal of Sound and Vibration 332 (2013) 867–893.
[28] A. R. Diaz, A. G. Haddow, L. Ma, Design of band-gap grid structures, Structural and Multidisciplinary Optimization 29 (2005) 418–431.
[29] S. Halkjar, O. Sigmund, J. S. Jensen, Maximizing band gaps in plate structures, Structural and Multidisciplinary Optimization 32 (2006) 263–275.
[30] W. Xiao, G. W. Zeng, Y. S. Cheng, Flexural vibration band gaps in a thin plate containing a periodic array of hemmed discs, Applied Acoustics 69 (2008) doi:10.1016/j.apacoust.2006.09.003.
[31] F. Farzbod, M. J. Leamy, Analysis of Bloch's method in structures with energy dissipation, Journal of Vibration and Acoustics, Transactions of the ASME 133 (2011) doi:10.1115/1.4003943.
[32] L. Liu, M. I. Hussein, Wave motion in periodic flexural beams and characterization of the transition between bragg scattering and local resonance, Journal of Applied Mechanics, Transactions ASME 79 (2012) doi:10.1115/1.4004592.
[33] T. Suzuki, P. K. L. Yu, Complex elastic wave band structures in three-dimensional periodic elastic media, Journal of the Mechanics and Physics of Solids 46 (1998) 115–138.
[34] S. V. Sorokin, O. A. Ershova, Plane wave propagation and frequency band gaps in periodic plates and cylindrical shells with and without heavy fluid loading, Journal of Sound and Vibration 278 (2004) 501–526.
[35] C. Charles, B. Bonello, F. Ganot, Propagation of guided elastic waves in 2D phononic crystals, Ultrasonics 44 (2006) doi:10.1016/j.ultras.2006.05.096.
[36] Y. Z. Wang, F. M. Li, W. H. Huang, X. Jiang, Y. S. Wang, K. Kishimoto, Wave band gaps in two-dimensional piezoelectric/piezomagnetic phononic crystals, International Journal of Solids and Structures 45 (2008) 4203–4210.
[37] M. J. Leamy, Exact wave-based Bloch analysis procedure for investigating wave propagation in two-dimensional periodic

MOST WIEDZY Downloaded from mostwiedzy.pl

lattices, Journal of the Mechanics and Physics of Solids 331 (2012) 1580–1596.
[38] F. Kobayashi, S. Biwa, N. Ohno, Wave transmission characteristics in periodic media of finite length: Multilayers and fiber arrays, International Journal of Solids and Structures 41 (2004) 7361–7375.
[39] A. L. Chen, Y. S. Wang, Study on band gaps of elastic waves propagating in one-dimensional disordered phononic crystals, Physica B: Condensed Matter 392 (2007) 369–378.
[40] D. Yu, Y. Liu, H. Zhao, G. Wang, J. Qiu, Flexural vibration band gaps in Euler-Bernoulli beams with locally resonant structures with two degrees of freedom, Physical Review B – Condensed Matter and Materials Physics 73 (2006) doi:10.1103/PhysRevB.73.064301.
[41] D. Yu, J. Wen, H. Zhao, Y. Liu, X. Wen, Vibration reduction by using the idea of phononic crystals in a pipe-conveying fluid, Journal of Sound and Vibration 318 (2008) 193–205.
[42] L. Liu, M. I. Hussein, Wave motion in periodic flexural beams and characterization of the transition between bragg scattering and local resonance, Journal of Applied Mechanics, Transactions ASME 79 (2012) doi:10.1115/1.4004592.
[43] M. Rahman, M. A. Stuchly, Circularly polarised patch antenna with periodic structure, IEE Proceedings: Microwaves, Antennas and Propagation 149 (2002) 141–146.
[44] P. F. Hsieh, T. T. Wu, J. H. Sun, Three-dimensional phononic band gap calculations using the FDTD method and a PC cluster system, IEEE Transactions on Ultrasonics, Ferroelectrics, and Frequency Control 53 (2006) 148–158.
[45] T. Lu, G. Gao, S. Ma, F. Jin, T. Kim, Acoustic band gaps in two-dimensional square arrays of semi-hollow circular cylinders, Science in China, Series E: Technological Sciences 52 (2009) 303–312.
[46] J. Shibayama, R. Ando, J. Yamauchi, H. Nakano, An LOD-FDTD method for the analysis of periodic structures at normal incidence, IEEE Antennas and Wireless Propagation Letters 8 (2009) 890–893.
[47] X. Q. Zhou, D. Y. Yu, X. Shao, S. Wang, Y. H. Tian, Band gap characteristics of periodically stiffened-thin-plate based on center-finite-difference-method, Thin-Walled Structures 82 (2014) 115–123.
[48] D. L. Thomas, Dynamics of rotationally periodic structures, International Journal for Numerical Methods in Engineering 14 (1979) 81–102.
[49] P. Langlet, A. C. Hladky-Hennion, J. N. Decarpigny, Analysis of the propagation of plane acoustic waves in passive periodic materials using the finite element method, Journal of the Acoustical Society of Americas 98 (1995) 2792–2800.
[50] M. Ruzzene, F. Scarpa, F. Soranna, Wave beaming effects in two-dimensional cellular structures, Smart Materials and Structures 12 (2003) 363–372.
[51] D. Duhamel, B. R. Mace, M. J. Brennan, Finite element analysis of the vibrations of waveguides and periodic structures, Journal of Sound and Vibration 294 (2006) 205–220.
[52] Y. Cheng, J. Y. Xu, X. J. Liu, Analysis of the propagation of plane acoustic waves in passive periodic materials using the finite element method, Physical Review B – Condensed Matter and Materials Physics 77 (2008) doi:10.1103/PhysRevB.77.045134.
[53] Z. J. Wu, F. M. Li, Y. Z. Wang, Study on vibration characteristics in periodic plate structures using the spectral element method, Acta Mechanica 224 (2013) 1089–1101.
[54] Y. Xiao, J. Wen, G. Wang, X. Wen, Theoretical and experimental study of locally resonant and bragg band gaps in flexural beams carrying periodic arrays of beam-like resonators, Journal of Vibration and Acoustics, Transactions of the ASME 135 (2013) doi:10.1115/1.4024214.
[55] Z. J. Wu, Y. Z. Wang, F. M. Li, Analysis on band gap properties of periodic structures of bar system using the spectral element method, Waves in Random and Complex Media 23 (2013) 349–372.
[56] Z. J. Wu, F. M. Li, Y. Z. Wang, Vibration band gap properties of periodic Mindlin plate structure using the spectral element method, Meccanica 49 (2014) 725–737.
[57] Z. J. Wu, F. M. Li, C. Zhang, Vibration band-gap properties of three-dimensional Kagome lattices using the spectral element method, Journal of Sound and Vibration 341 (2015) 162–173.
[58] J. O. Vasseur, P. A. Deymier, G. Frantziskonis, G. Hong, B. Djafari-Rouhani, L. Dobrzyński, Experimental evidence for the existence of absolute acoustic band gaps in two-dimensional periodic composite media, Journal of Physics Condensed Matter 10 (1998) 6051–6064.
[59] T. Miyashita, Sonic crystals and sonic wave-guides, Measurement Science and Technology 16 (2005) doi:10.1088/0957–0233/16/5/R01.
[60] T. C. Wu, T. T. Wu, J. C. Hsu, Waveguiding and frequency selection of lamb waves in a plate with a periodic stubbed surface, Physical Review B – Condensed Matter and Materials Physics 79 (2009) doi:10.1103/PhysRevB.79.104306.
[61] Y. Pennec, J. O. Vasseur, B. Djafari-Rouhani, L. Dobrzyński, P. A. Deymier, Two-dimensional phononic crystals: Examples and applications, Surface Science Reports 65 (2010) 229–291.
[62] M. Airoldi, L. Ruzzene, Piezoelectric superlattices and shunted periodic arrays as tunable periodic structures and metamaterials, Wave Propagation in Linear and Nonlinear Periodic Media: Analysis and Applications Springer Vienna (2012) 33–108.
[63] S. M. Jeong, M. Ruzzene, Experimental analysis of wave propagation in periodic grid-like structures, Proceedings of SPIE - The International Society for Optical Engineering 5760 (2005) 518–525.
[64] M. Oudich, M. Senesi, M. B. Assouar, M. Ruzenne, J. H. Sun, B. Vincent, Z. Hou, T. T. Wu, Experimental evidence of locally resonant sonic band gap in two-dimensional phononic stubbed plates, Physical Review B – Condensed Matter and Materials Physics 84 (2011) doi:10.1103/PhysRevB.84.165136.
[65] A. Oseev, R. Lucklum, M. Ke, M. Zubtsov, R. Grundmann, Phononic crystal sensor for liquid property determination, Proceedings of SPIE - The International Society for Optical Engineering 8346 (2012) doi:10.1117/12.914783.
[66] P. Celli, S. Gonella, Manipulating waves with LEGO® bricks: A versatile experimental platform for metamaterial architectures, Applied Physics Letters 107 (2015) doi:10.1063/1.4929566.

MOST WIEDZY Downloaded from mostwiedzy.pl

[67] J. Wu, X. C. Bai, Y. Xiao, M. X. Geng, D. L. Yu, J. H. Wen, Low frequency band gaps and vibration reduction properties of a multi-frequency locally resonant phononic plate, Acta Physica Sinica 65 (2016) doi:10.7498/aps.65.064602.
[68] A. Żak, M. Krawczuk, M. Palacz, Periodic properties of 1D FE discrete models in high frequency dynamics, Mathematical Problems in Engineering 2016 (2016) doi:10.1155/2016/9651430.
[69] W. Ostachowicz, P. Kudela, M. Krawczuk, A. Żak, Guided Waves in Structures for SHM. The Time-domain Spectral Element Method, John Wiley & Sons Ltd., Singapore, 2012.
[70] O. C. Zienkiewicz, The Finite Element Method, McGraw-Hill Book Company, London, 1989.
[71] A. Żak, M. Krawczuk, Assessment of flexural beam behaviour theories used for dynamics and wave propagation problems, Journal of Sound and Vibration 331 (2012) 5715–5731.
[72] R. D. Blevins, Formulas for Natural Frequency and Mode Shapes, Krieger Publishing Company, Amsterdam, 1976.
[73] R. A. Schapery, A theory of mechanical behaviour of elastic media with growing damage and other changes in structure, Journal of the Mechanics and Physics of Solids 38 (1990) 215–253.
[74] J. Lemaitre, J. L. Chaboche, Mechanics of Solid Materials, Cambridge University Press, Cambridge, 1990.
[75] J. Lemaitre, A Course of Damage Mechanics, Springer-Verlag, Inc., Berlin, 1992.
[76] C. Tofallis, A better measure of relative prediction accuracy for model selection and model estimation, Journal of the Operational Research Society 66 (2015) 1352–1362.
[77] L. Brillouin, Wave propagation in periodic structures, electric filters and crystal laticies, Dover Publications, Inc., New York, 1946.
[78] P. A. Kuchment, Floquet theory for partial differential equations, Russian Mathematical Surveys 37 (1982) 1–60.
[79] C. Kittel, Introduction to solid state physics, John Wiley & Sons, Inc, New York, 2005.
[80] A. Żak, M. Krawczuk, Ł. Skarbek, M. Palacz, Numerical analysis of elastic wave propagation in unbounded structures, Finite Elements in Analysis and Design 90 (2014) 1–10.
[81] J. F. Doyle, Wave Propagation in Structures, Springer-Verlag, Inc., New York, 1997.

MOST WIEDZY Downloaded from mostwiedzy.pl